Engineered Science

RESEARCH PAPER

View Article Online

Functionalization and Fabrication of Soluble Polymers of Intrinsic Microporosity for CO_2 Transformation and Uranium Extraction

Anwang Dong, Tingting Dai, Mengyao Ren, Xuemei Zhao, Shilei Zhao, Yihui Yuan, Qi Chen* and Ning Wang*

Task-specific porous polymer PIM-1-based quaternary ammonium iodide (**PIM-1-AI**) with available catalytic site has been obtained by functionalization of the precursor polymer of intrinsic microporosity PIM-1 and used in the capture and fixation of CO_2. **PIM-1-AI** not only have the ability to capture CO_2 (4.6 wt%, 273 K), but also can act as metal-free catalyst for CO_2 conversion reaction without any co-catalyst to prepare various cyclic carbonates. The yields of the corresponding reactions catalyzed by **PIM-1-AI** range from 87 % to 99 % at 2.5 MPa and 90 °C. Furthermore, post-functionalization of PIM-1 has also been performed for the synthesis soluble PIM-1-based amidoxime (**PIM-1-AO)** with adsorbent groups and high BET specific surface area (511 $m^2 g^{-1}$). Given that the inevitable mass loss of solid powder absorbents in the process of recycling and reutilization for practical use, herein, solid powder **PIM-1-AO** was fabricated into film and foam-supporting monolithic adsorbents to meet the need of practical application for uranium uptake. We found that **PIM-1-AO** film has the highest uranium uptake ability (180.3 mg g^{-1}) tested in real seawater with evaluated uranium (7.98 ppm) at the pH of 8.2 and room temperature. Foam-supporting **PIM-1-AO** can shorten the balanced time from 10 to 4 h in compare with **PIM-1-AO** powder. Moreover, both **PIM-1-AO** film and foam-supporting **PIM-1-AO** as integrated adsorbents can be reused at least 5 times and retain their mass stability.

Keywords: Polymer of intrinsic microporosity; Fabrication; CO_2 uptake and fixation; Film; Sponge; Uranium extraction

Received 9 October 2018**, Accepted** 10 November 2018

DOI: 10.30919/es8d613

1 Introduction

The growing emission of greenhouse gas carbon dioxide (CO_2) has caused a set of problems to environment and human beings during the booming process of industrialization and urbanization.[1] Although CO_2 has been chemically adsorbed in the industry, the large amount of energy consumed in this process, remains an barrier from an economic point of view.[2] Therefore, massive adsorbents from inorganic materials to organic materials and organic-inorganic hybrid materials have been employed to pre-combustion or post-combustion CO_2 capture.[3-5] Among them, the porous organic polymers (POPs) as the solid sorbents for CO_2 have irreplaceable advantages owing to the less energy required both in the capture and release CO_2.[2,6-8] However, from the long-term and resource saving perspectives, the CO_2 adsorbed followed by being buried in the ground can't meet the long run development of society.[9-11] An alternative avenue is the CO_2 utilization, that is, the CO_2 fixation and transformation reaction using renewable, sustainable, nonflammable, and well-sourced CO_2 replacing CO[12] as C1 feedback to afford high value-added products, such as cyclic carbonates,[13,14] methanol,[15,16] and urea.[1,17] Whereas, CO_2 is sluggish reactivity both in thermodynamics and kinetics owing to the carbon atom of CO_2 being in the highest valence state.[18,19] In this regard, elevated attempt has been devoted to exploiting and designing efficient, green, and non-toxic catalysts including metal complex (such as, main group,[20-23] and transition[24-27] metal) and organics (for example, organic superbase,[28-31] and POPs[10,32-35]) to remove this bottleneck and realize 100 % atom involved reaction. Among these catalysts, POPs are promising ones in view of the growing requirement of the purity of the corresponding products without any metal residue.

Environmental problems, such as global warming, caused by traditional fossil fuel combustion are driving the increasing development of a great number of low-carbon and carbon-free energy, such as solar energy, water–based energy and nuclear energy.[36-38] Nevertheless, the growth of those new energy has a lot of difficulties, such as the shortage of uranium raw material and contamination of nuclear waste liquid for nuclear energy.[39-41] The uranium content of seawater is about 99 % (approximate 40 million tons) of the total, but at the extremely low concentration (about 3.3 ppb), which leads to considerable works for uranium extraction in the seawater.[42-44] Moreover, real seawater, unlike simulated seawater or pure water, has more complex components, like many trace elements not just uranium, microorganisms, and plants.[41,45] Given that POPs can be modified after synthesis to give specific functionality.[46,47] Especially, POPs with amidoxime groups show good performance in uranium capture in the seawater with a large amount of uranium raw material meeting the requirement for sustainable development of carbon-free nuclear energy, as well as nuclear waste liquid with long-lived, non-biodegradable but residual uranium metal ion doing harm to water and human health.[48-51] These POPs have the chemically and thermodynamically stable structure as well as good chelation for uranium, and thereby can be reused and recycled in uranium extraction several times. However, the inevitable loss of some mass of these solid powder absorbents in the process of recycling and reutilization remains a problem. Meanwhile, these amidoxime-modified POPs sorbents without solubility or processability, which therefore are barriers for real application.

State Key Laboratory of Marine Resource Utilization in South China Sea, Hainan University, Haikou 570228, P. R. China
***E-mail:** chenqi@hainu.edu.cn ; wangn02@foxmail.com*

To realize both CO_2 capture and transformation as well as solve the above-mentioned barriers, a well-known PIM with solubility was employed and further be tailored to give two functional polymers. As one class of POPs, PIMs with permanent microporous structure and high specific surface area can be processed in some organic solvents as well as prepared in a large scale, owing to the inefficient packing of molecular chains and linear but not reticular molecular structure.[52-54] Inspired by this and based on our experience with POPs[55-57], in this work, the PIM-1 was opted as the precursor and two post-functionalization means were employed to afford PIM-1-based quaternary ammonium iodide (**PIM-1-AI**) with availably catalytic site and PIM-1-based amidoxime (**PIM-1-AO)** with adsorbent groups. **PIM-1-AI** was tested of the CO_2 capture ability and researched as meatal-free catalyst without any co-catalyst via the most common fixation reaction for the synthesis of various cyclic carbonates using CO_2 and the relevant epoxides as the feedbacks. **PIM-1-AO** was further made into film and supported by melamine sponge to firstly give two integrated adsorbents. The three of them were employed in the uranium extraction in evaluated uranium concentration (7.98 ppm) real seawater at the pH of 8.2 and room temperature, and their relevant performance coupled with mass stability during the reused course were contrasted adequately. To the best of our knowledge, **PIM-1-AI** is the first example of PIMs used for both CO_2 capture and fixation, otherwise**, PIM-1-AO** is also firstly fabricated into film and foam-supporting monolithic adsorbents for practical application of uranium extraction.

2 Experimental Section

2.1 Materials

Hydroxylamine aqueous solution (50 %), sodium hydroxide (96 %), 5,5',6,6'-Tetrahydroxy-3,3,3',3'-tetramethylspirobisindane (97 %), and iodomethyl trimethylammonium iodide (98 %) were purchased from Alfa Aesar Co., Ltd. Ammonium chloride (99 %) was obtained from Heng xing chemical preparation Co., Itd. Tetrafluoroterephthalonitrile (99 %), potassium carbonate (99 %), tetrabutylammonium iodide (TBAI, 99 %), and uranyl nitrate hexahydrate (99 %) were obtained from Macklin Co., Ltd. Sodium azide (99 %), and all the epoxides (99 %) were obtained from Aladdin Reagent Co., Ltd. All Anhydrous reagents, such as, tetrahydrofuran (THF, 99.5 %), dichloromethane (DCM, 99.9 %), ethanol (99.5 %), methanol (99.9 %) and N, N-Dimethylformamide (DMF, 99.8 %) were commercially available from Macklin Co., Ltd. All the chemical substances and reagents described above are used as originally received.

2.2 Synthesis of polymers

Preparation of PIM-1: PIM-1 was obtained via the reported means.[58-60] Briefly, in a 100 ml round bottom flask, 5,5',6,6'-Tetrahydroxy-3,3,3',3'-tetramethylspirobisindane (3.1 g, 9.0 mmol), tetrafluoroterephthalonitrile (1.8 g, 9.0 mmol), and anhydrous potassium carbonate (2.5 g, 18.0 mmol) were dissolved in dry DMF (60 ml), then the mixture was stirred at 70 °C for 3 days in oxygen-free atmosphere. After cooling and filtering, the crude product was washed with excessive water and methanol to eliminate the residual small molecule reactants or unwanted but obtained oligomer. Finally, the pure polymer PIM-1 (4.0 g, 95 %) was isolated as yellow solid powder after a further purification process, namely, Soxhlet extraction with methanol for 12 h.

Preparation of PIM-1-AI: To prepare **PIM-1-AI**, the intermediate product **PIM-1-TZ** was firstly customized by modifying the predecessor PIM-1 via a more advanced method in comprise with the reported procedure.[61] To be brief, in a 250 ml round bottom flask, a mixture of PIM-1 (500 mg), sodium azide (1.4 g, 21.9 mmol) and ammonium chloride (1.2 g, 21.7 mmol) were dissolved in DMF (80 ml), then stirred at 120 °C under the argon atmosphere for 60 h to adequately transform the cyano groups to tetrazole groups. After cooling, the precipitate was obtained by the addtion of the 100 ml of dilute hydrochloric acid (0.3 mol L^{-1}) dropwise. Then the solution was centrifugated and washed repeatedly by water to remove the unwanted materials. Finally, the immediate product **PIM-1-TZ** (570 mg, 96 %) was tailored after drying for 24 h.

After the synthesis of **PIM-1-TZ**, in a 100 ml round bottom flask, a mixture of **PIM-1-TZ** (300 mg) and anhydrous potassium carbonate (182 mg, 1.3 mmol) were dissolved in DMF (50 ml) and stirred at the room temperature for 0.5 h. Then the solution was heated to 60 °C and iodomethyl trimethylammonium iodide (538 mg, 1.7 mmol) dissolved in DMF (2 ml) was added drop by drop, followed by being stirred at this temperature for 24 h. After cooling, the solution was poured into a dialysis tube, then placed into a beaker (2L) filled with repleaded repeatedly water, to fully remove the residual reactant. Finally, the **PIM-1-AI** (351 mg, 65 %, based on **PIM-1-TZ**) was obtained as light-yellow solid powder after being cooled in a freeze dryer for 36 h.

Preparation of PIM-1-AO: PIM-1 (200 mg) and anhydrous potassium carbonate （200 mg, 1.5 mmol）were dissolved in the mixture of hydroxylamine aqueous solution (5.0 mL) and THF (20 ml), then stirred at 69 °C under condensing for 36 h to modificate PIM-1. After being cooled down to 30 °C, the mixed solution was filterd and washed iteratively by water and methanol to remove the superfluous starting materials. Finally, the modified PIM-1 as white solid powder, namely, **PIM-1-AO** (221 mg, 97 %, based on PIM-1) was obtained after drying for 36 h.

Preparation of PIM-1-AO film: **PIM-1-AO** (40 mg) was fully dissolved in DMF (3 ml) under the role of ultrasound, then the mixed solution was poured into a glass-state petri dish (3.5 cm diameter). Finally, the light-yellow solid membrane named **PIM-1-AO** film was prepared after drying in vacuum for 4 days to slowly evaporate the solvent DMF.

***Preparation of foam-supporting PIM-1-AO*:** Melamine foam (9 mg) was wrapped with the DMF (3 ml) solution of **PIM-1-AO** (400 mg). Then the mixture was placed in vacuum for 3 days to slowly evaporate the solvent DMF to give an integrated and stable foam-supporting **PIM-1-AO** (389 mg).

2.3 Characterization and measurement

^1H spectra of the polymers were analyzed on a Bruker DMX400 NMR spectrometer. The FT-IR spectra of all the prepared polymers were recorded by using a PerkinElmer FT-IR spectrometer under normal conditions. The microscopic structures of the polymers were observed by a Hitachi S-4800 scanning electron microscope (SEM). X-ray photoelectron spectroscopy (XPS) of all the polymers were carried out on a Kratos AXIS SUPRA spectrometer. Thermogravimetric analysis (TGA) of all the materials was studied by a NETZSCH STA 449 F3 TGA simultaneous thermal analyzer under a nitrogen atmosphere and at a heating speed of 10 °C min^{-1} from room temperature to 900 °C. Nitrogen gas (N_2) and CO_2 sorption isotherms were measured by a Micromeritics ASAP 2460 physical adsorption instrument. The BET specific surface area was evaluated based on the obtained adsorption−desorption isotherms in the relative pressure (P/P_0) ranging from 0.01 to 0.1. The PSD profiles of the polymers were calculated from the related adsorption branches by the nonlocal density function theory (NLDFT) approach. The total pore volume was calculated from nitrogen adsorption−desorption isotherms at $P/P_0 = 0.99$.

2.4 Studies on catalytic fixation of CO_2

The catalytic test was performed in a reactor (50 ml) filled with CO_2 (2.5 MPa) at 90 °C. All the tests are similar, one catalyst (0.1 mol%, calculation based on the repeating unit) and one epoxide were added into the reactor, then the gas in the reactor was changed by CO_2 (2.5 MPa) for three times to obtain a pure CO_2 atmosphere (2.5 MPa) at 0 °C. Then the reactor was stirred at 90 °C for a certain time (such as 4 h), after cooling to 25 °C, the CO_2 in the reactor was discharged. The mixture was filtered and washed by DCM, then column chromatography was performed to further purify and separate the desired product from the concentrated filtrate. The product yield can be calculated based on the isolated product or determined by ^{1}H NMR. As for the repeatability test, the recycled catalyst was obtained by filtering, washing and drying, then reused as a new catalyst in the next run.

2.5 Uranium extraction studies

The evaluated uranium solution (7.98 ppm, pH=8.2) was configured by the adjustment of uranyl nitrate hexahydrate, negligible and diluted hydrochloric acid and sodium hydroxide, and filtered real seawater. In a representative experiment, the adsorbent (**PIM-1-AO**, **PIM-1-AO** film, foam-supporting **PIM-1-AO**, 5 mg) and the 500 ml of the excess uranium solution were poured into a plastic bottle, then the bottle was rocked at the 100-rpm speed in a shaker. The measurement of uranium concentration and uptake performance of the adsorbents are similar to the reported means.[62,63]

Regeneration of the polymer adsorbent: After each run of uranium adsorption, the adsorbent was desorbed with potassium hydroxide (0.75 M), then filtered and washed by ultrapure water and methanol repeatedly. After being dried in vacuum for 24 h, the regenerated polymer adsorbent was obtained and used for next adsorption experiment cycle. The experiment conditions are basically consistent with the above-mentioned uranium uptake studies, the slight difference is that the adsorbent mass is not always 5 mg but the ratio of adsorbent and uranium solution is constant (1mg: 100 ml).

3 Results and Discussion

3.1 Preparation and characterization

Synthetic route for preparation of **PIM-1-AO** and **PIM-1-AI** from PIM-1 was displayed in Scheme 1. The well-known PIM-1[58] possessing the permanent micropore structure, high specific surface area, and solution processability was selected as the precursor and further modified to the target polymers. Treatment PIM-1 containing cyano groups with hydroxylamine aqueous solution and potassium carbonate in refluxing THF can afford **PIM-1-AO** with amidoxime groups in high yield. As for the post-modification to **PIM-1-AI**, the intermediate product PIM-1-TZ possessing the permanent micropore structure and high absorption capacity for CO_2 was obtained in the first step by cycloaddition of PIM-1 with NaN_3 according to a more advanced method in comprise with the reported procedure.[61] In this [2 + 3] cycloaddition reaction that is 'click chemistry', ammonium chloride not zinc chloride reported in previous literature was employed as the catalyst, showing that ammonium chloride is also a reliable metal-free catalyst for the reaction. And then, quaternary ammonium iodide was grafted onto the tetrazole moieties of **PIM-1-TZ** by treatment with iodomethyl trimethylammonium iodide and potassium carbonate in DMF to give the desired polymer **PIM-1-AI**.

The structures of PIM-1, **PIM-1-AI** and **PIM-1-AO** were firstly certified by comparative FTIR spectra. The typical absorption peak of cyano groups in PIM-1 is located at 2240 cm^{-1} from the corresponding IR data shown in Fig. 1a.[62] After functionalization, the disappearance of cyano groups stretching bands was found for **PIM-1-AI** and **PIM-1-**

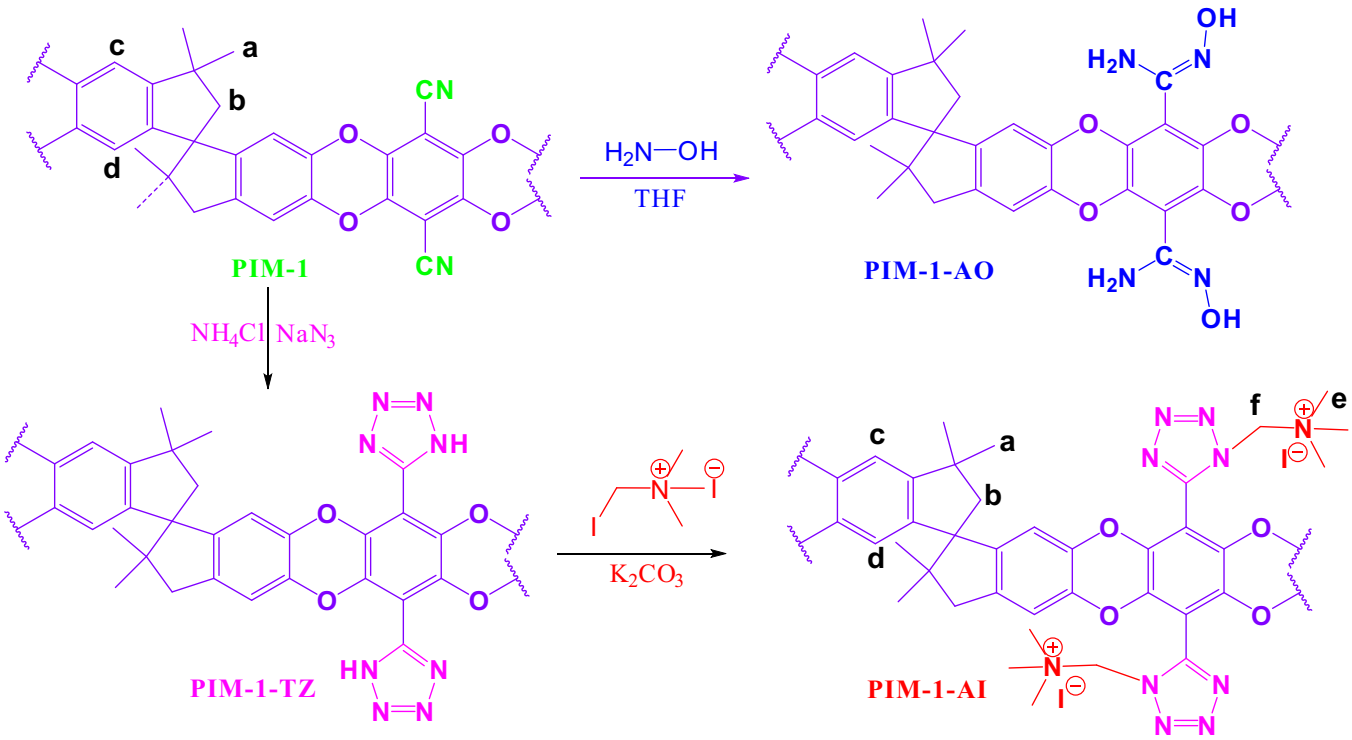

Scheme 1. Post-functionalization of PIM-1 to **PIM-1-AO** and **PIM-1-AI**.

AO. Besides, a new peak band at about 1640 cm^{-1} could be ascribed to tetrazole adsorption vibration in **PIM-1-AI**, and the stronger board peak at about 3450 cm^{-1} could be corresponded to the existence of water or unreacted tetrazole N-H in **PIM-1-AI**.[61] For **PIM-1-AO**, the emerging peaks at 1657, 3387 and 3485 cm^{-1} could be attributed to the stretching band of -C=N-, -OH, and -NH_2 in amidoxime groups, respectively.[64] ^{1}H NMR spectrum was also performed to characterize **PIM-1-AI**. By contrast spectra of PIM-1 in $CDCl_3$ and **PIM-1-AI** in d_6-DMSO in Fig. 1b, the presence of expected signal peaks for **PIM-1-AI** at 4.09 (-NCH_3) and 4.54 (-NCH_2-) ppm derived from iodomethyl trimethylammonium iodide clearly confirm that quaternary ammonium iodide was successfully linked to the polymer by post-modification.

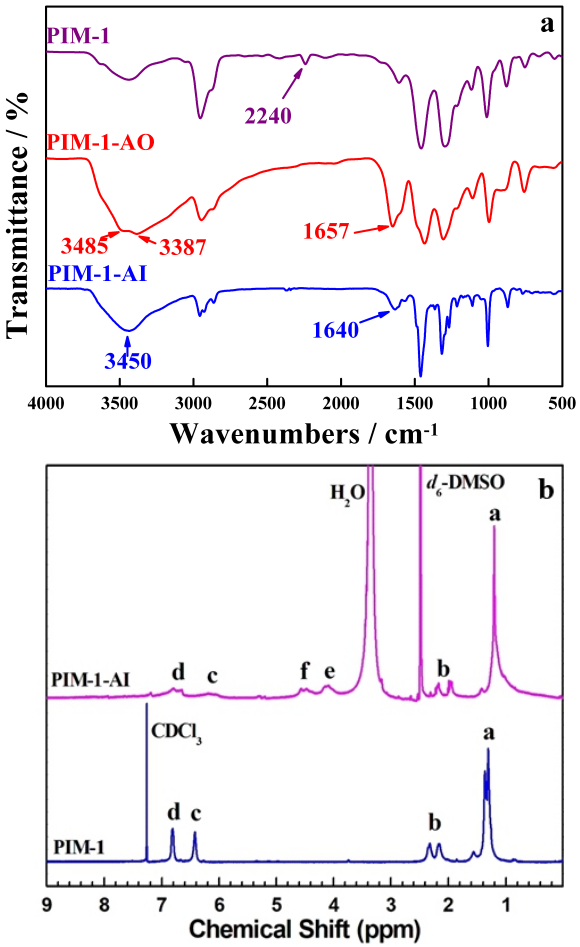

Fig. 1 (a) FTIR spectra of the polymers **PIM-1**, **PHN-2-AO** and **PIM-1-AI**. **(b)** ^{1}H NMR spectra of **PIM-1** and **PIM-1-AI**.

The XPS spectra measurement was employed to further characterize the structure of the polymers. As evidence from Fig. 2a, the signal peaks at 620.7 eV ($I3d_{5/2}$) and 632.4 eV ($I3d_{3/2}$) of **PIM-1-AI** XPS spectra indicate the existence of iodine ion. Moreover, the nitrogen species in the polymers were demonstrated in Figs. 2b-d. The original N1s peak located at 399.0 eV is stemmed from the cyano groups of PIM-1. After modification, the N1s signal peaks of both **PIM-1-AI** and **PIM-1-AO** have remarkable change. Consequently, the nitrogen species of **PIM-1-AI** and **PIM-1-AO** were curve-fitted into a number of peaks based on diverse composition of nitrogen atom for charity. The N1s peak of **PIM-1-AI** was also located at a higher bonding energy in contrast to PIM-1 and can be distributed into four species of the newly formed tetrazole ring including C-*N*H-N (398.9 eV), N=N-*N* (399.6 eV), N-*N*=N (400.2 eV), and C=*N*-N (400.8 eV) as well as one specie of the quaternary ammonium iodide moiety CH_2-*N*-$(CH_3)_3$ (401.6 eV). The N1s peak of **PIM-1-AO** is at a higher bonding energy in contrast to PIM-1 and can be distributed into two species of C=*N*-OH (399.5 eV) and C-*N*H_2 (398.9 eV) derived from amidoxime groups of the polymer.

To study the porous features of the polymers **PIM-1-AI** and **PIM-1-AO**, the N_2 adsorption and desorption isotherms were tested at 77 K. As shown in Fig. 3a, the three materials as typical microporous substances demonstrate the similar sorption curve attributed to type I isotherm, which is the sharp N_2 adsorb at low relative pressure, followed by a gentle addition of N_2 adsorption amount with the increasing relative pressure.[65] Furthermore, their adsorption and desorption isotherms are noncoincidence and the presence of hysteresis loops indicate that all polymers also possess mesoporous structure.[47,66] The PSD profiles of polymers shown in Fig. 3b were definitely demonstrated the size of pore diameter of polymers. We can see that most of the pore size of all the polymers are less than 2 nm. Other important porosity features of the polymers were exhibited in Table 1. The BET specific surface area (S_{BET}) value of PIM-1 is 724 $m^2 g^{-1}$, after post-modification, the value of **PIM-1-AI** and **PIM-1-AO** is decreased to 154 $m^2 g^{-1}$ and 511 $m^2 g^{-1}$, respectively.

The thermodynamic stability of the polymers **PIM-1-AI** and **PIM-1-AO** was investigated based on the TGA curves measured in the N_2 atmosphere (Fig. S1). Compared to the stable precursor PIM-1, which shows high decomposition temperature at about 500 °C, post-modification to **PIM-1-AI** and **PIM-1-AO** leads to decrease of decomposition temperature at about 250 °C and 50 % loss mass at 800 °C. The expected lower decomposition temperature of **PIM-1-AI** or **PIM-1-AO** might be attributed to the decomposition of tetrazole group and quaternary ammonium iodide moieties or amidoxime groups when the temperature is up to 250 °C.

The nitrogen-containing porous polymers with light density, high affinity to CO_2 and good recyclability have been proven as promising carbon capture and storage (CCS) adsorbents.[6-8,24] In addition, the quaternary ammonium iodide was opted as the active catalysts for synthesis of high value-added cyclic carbonates from epoxides and CO_2.[24] Thus, the quaternary ammonium iodide was attached onto the tetrazole-decorated polymer PIM-1-TZ that has been proven to have good carbon dioxide adsorption properties to produce **PIM-1-AI**, which we presume as the task-specific, metal-free polymeric catalyst to capture and transform CO_2 under the mild condition without any co-catalyst. Before the catalytic study, the CO_2 uptake performance of PIM-1 and **PIM-1-AI** were measured at 273 K as shown in Fig. 4. Though the BET specific surface area of **PIM-1-AI** decreases 80 % from the precursor **PIM-1** to 154 $m^2 g^{-1}$, its CO_2 uptake capacity at 1 bar and 273 K is still 4.6 wt%, which is more than 55 % of the precursor PIM-1.

The corresponding CO_2 transformation to cyclic carbonates from a series of substituted epoxides catalyzed by different catalysts was performed at 2.5 MPa and 90 °C. The involved results were demonstrated in Table 2 and the possible mechanism coupled with details were shown in the Supporting Information (Fig. S2). The $PhOCH_2$ substituted epoxide was firstly opted for preparing the corresponding cyclic carbonate to verify the catalytic performance of the catalysts PIM-1, **PIM-1-AI** and TBAI. Under the given conditions and 4h reaction time, only trace cyclic carbonates can been obtained using PIM-1 as catalyst or without any catalyst (Entries 1-2). By contrast, when TBAI acts as the catalyst, the yield is increased to 36 % (Entry3). However, for catalyst **PIM-1-AI** (Entry 4), the relevant yield is the best and up to 75 % determined by ^{1}H NMR (Fig. S3). Inspired

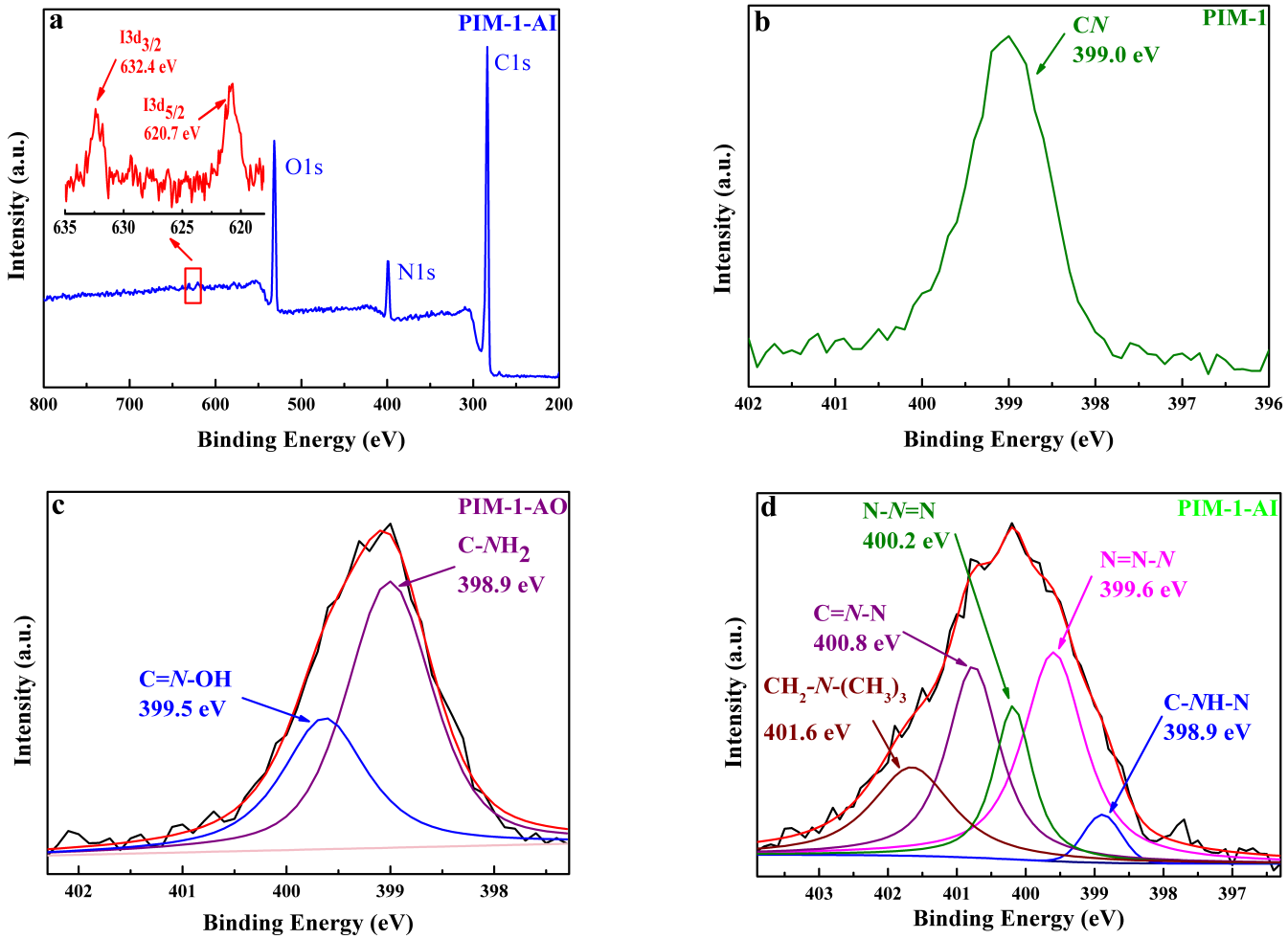

Fig. 2 The wide scan XPS spectra of PIM-1-AI (a) and the high resolution N1s XPS spectra (b for PIM-1, c for PIM-1-AO, and d for PIM-1-AI).

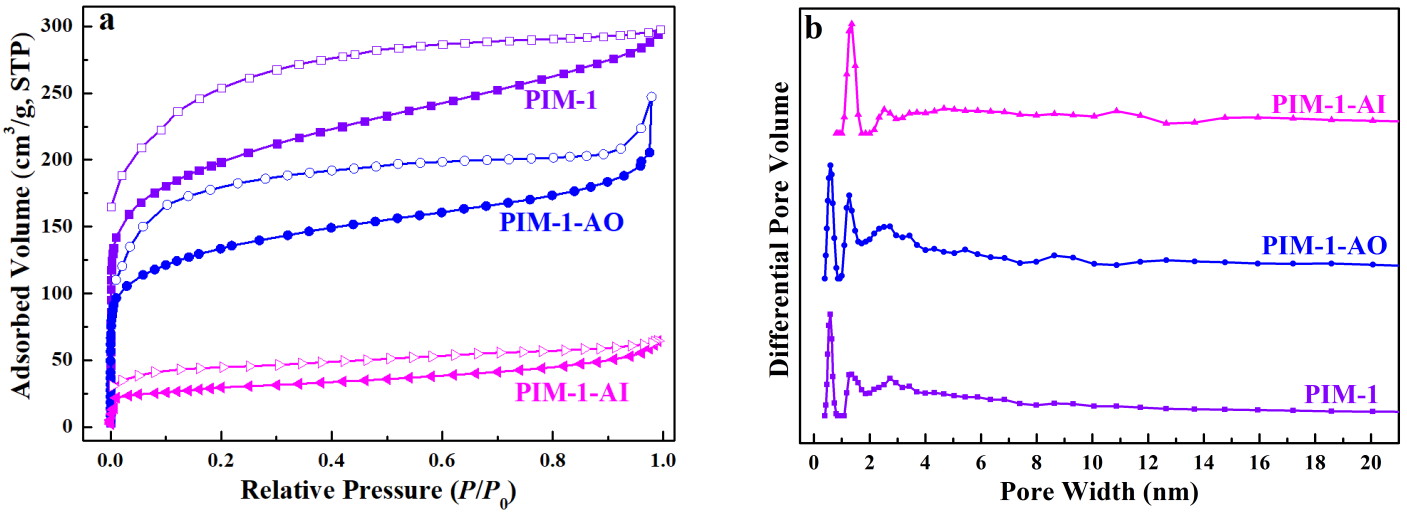

Fig. 3 (a) Nitrogen adsorption–desorption isotherms of the polymers PIM-1, **PIM-1-AO** and **PIM-1-AI** measured at 77 K. The adsorption and desorption curves are marked with solid and open symbols, respectively. **(b)** PSD profiles of the polymers PIM-1, **PIM-1-AO** and **PIM-1-AI** calculated by NLDFT.

Table 1 Porosities and CO_2 uptake capacities of polymers.

Polymers	S_{BET} [a] (m^2g^{-1})	V_{total} [b] (cm^3g^{-1})	D_{pore} [c] (nm)	CO_2 uptake [d] (wt%)
PIM-1	724	0.48	0.59,1.36-2.73	8.1
PIM-1-AO	511	0.40	0.59,1.27-2.51	-
PIM-1-AI	154	0.13	1.36	4.6

[a] Specific surface area calculated from the nitrogen adsorption isotherm using the BET method. [b] Total pore volume at P/P_0=0.99. [c] Date calculated from nitrogen adsorption isotherms with the NLDFT method. [d] Date were obtained at 1.0 bar and 273 K.

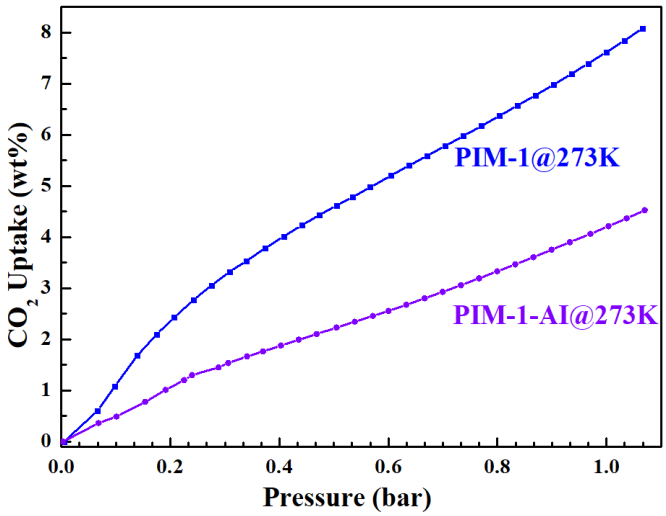

Fig. 4 CO_2 **uptake of** PIM-1 **and PIM-1-AI tested from 0 to 1 bar at 273**K.

by the high catalytic activity of **PIM-1-AI**, the reaction time was extended and the highest yield was up to 93 % after 6 h (Entry 5). To further prove **PIM-1-AI** can act as an effective catalyst for promotion of the CO_2 transformation reaction, other three epoxides with different substitutes (Ph, $ClCH_2$, and Me) were also employed as the starting compounds to react with CO_2 for preparing the corresponding cyclic carbonates. We can see that all the yields are higher than 85 % (Entries 6-8), especially quantitative transformation was found for methyl epoxide (Entry 8). As for repeatability test, the recycled catalyst **PIM-1-AI** was obtained by filtering, washing and drying, so that can be reused as a new catalyst in the next run. Based on our study, it can maintain effective catalytic capability after 5 cycles, demonstrating that **PIM-1-AI** is an economical catalyst.

In virtue of the soluble ability of **PIM-1** and amidoxime-based POPs have chelating ability with uranium.[41,44] The precursor PIM-1 was modified to give polymer **PIM-1-AO** with amidoxime groups and solubility, which can be considered as the alternative adsorbents for uranium extraction. Additionally, to avoid the loss of mass of the solid-state powder adsorbent (**PIM-1-AO**) in the recycling process like the reported sorbents, the polymer was further fabricated into film and processed onto melamine sponge as shown in Scheme 2 to afford two adsorbents meeting the need of practical application for uranium uptake. **PIM-1-AO** still keeps the solubility after post-modification, soluble in DMF, but insoluble in DCM, THF, MeOH. **PIM-1-AO** film was prepared by casting in the plate and then evaporate the DMF solution in vacuum. **PIM-1-AO** can also be coated onto melamine sponge to give another integrated adsorbent. The successfully obtained foam-supporting **PIM-1-AO** can be verified in the FTIR spectrum shown in the Fig. S4. The SEM image (Fig. S5) also shows that foam-supporting **PIM-1-AO** becomes more rougher than that of melamine sponge, giving a key evidence for the successful coating, that is, the **PIM-1-AO** has been successfully immobilized on melamine sponge.

To contrast and verify the practical application of uranium extraction in seawater of amidoxime-modified materials **PIM-1-AO**, **PIM-1-AO** film and foam-supporting **PIM-1-AO**, the uranium uptake measurements employing real seawater containing 7.98 ppm uranium, but not simulated seawater or distilled water, were performed at pH of 8.2 and room temperature. The uranium uptake ability of them were demonstrated in Fig. 5a, based on the corresponding uranium concentration curves shown in the inset. The balanced and saturated uranium uptake of **PIM-1-AO**, **PIM-1-AO** film and foam-supporting **PIM-1-AO** are 161.2, 180.3 and 159. 1 mg g^{-1}, respectively. Comparison of the maximum uranium uptake performance in this work with other POPs has been shown in Table S1 in the supporting information. We can see that **PIM-1-AO** film prepared in this work possesses higher uranium uptake performance compared with some other kinds of porous polymer reported before. Uranium uptake performance of **PIM-1-AO** film has a longer saturation time (12 h) but considerable enhancement of uranium uptake (11.85 %) compared with **PIM-1-AO** (10 h) as dispersed solid powder. As a monolithic adsorbent, the maximal uranium extraction of foam-supporting **PIM-1-AO** (159.1 mg g^{-1}) is competitive with the counterpart **PIM-1-AO** without any support, and as expected, it can shorten the saturation time from 8 to 4 h, which may because the enrichment effort of melamine sponge makes functional groups contact with uranium faster than before. More importantly, in the chelation between them and uranium, the O atom of N-*O*H and the N atom of C-*N*H_2 work together in the chelating adsorption process. To be more intuitive, the chelating schema of **PIM-1-AO** for uranium was illustrated in Fig. 5b, which is

Table 2 Studies on the catalytic transformation of CO_2

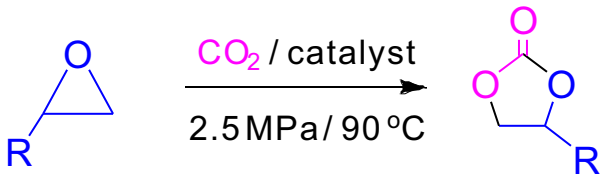

Entry	R	Catalyst	Time (h)	Yield %
1	$PhOCH_2$	no catalyst	4	Trace
2	$PhOCH_2$	PIM-1	4	Trace
3	$PhOCH_2$	TBAI	4	36
4	$PhOCH_2$	PIM-1-AI	4	75
5	$PhOCH_2$	PIM-1-AI	6	93
6	Ph	PIM-1-AI	6	87
7	$ClCH_2$	PIM-1-AI	6	95
8	CH_3	PIM-1-AI	6	99
9	CH_3	PIM-1-AI^{3rd}	6	99
10	CH_3	PIM-1-AI^{5th}	6	99

correspond with one of the common patterns reported previously.[69]

Though many adsorbents as solid power for uranium uptake can be recovered and reused several times, these kinds of sorbents have difficulty in practical use owing to their insoluble nature making them hard for processing, and as adsorbents, they have inevitable mass loss in the recycling and reusing procedure. Recyclability tests of the two sorbents **PIM-1-AO** film and foam-supporting **PIM-1-AO** as well as **PIM-1-AO** were employed to further demonstrate the performance of uranium extraction. After the uranium uptake tests, all of them were treated with NaOH (0.75 M) and washed to afford reused materials used as the new adsorbents in the next run measurement. The relevant results were shown in Fig. S6, by contrast, all of them can be recycled at least 5 times and retain their uranium uptake performance. However, the mass of **PIM-1-AO** reduced from 100 % to 31 % during the 5 times recyclability rests, only **PIM-1-AO** film and foam-supporting **PIM-1-AO** can retain their mass (Fig. S7) during the recycling and reusing procedure make them superior to **PIM-1-AO** existing as solid powder form for real application.

4. Conclusion

In this contribution, the polymer of microporosity PIM-1 with solubility and specific surface area 724 m^2 g^{-1} was opted as the precursor to produce two new polymers **PIM-1-AI** and **PIM-1-AO** by post-modification. **PIM-1-AI** containing quaternary ammonium iodide bearing tetrazole not only have the ability to capture CO_2 (4.6 wt%, 273 K), but also can act as metal-free catalyst without any co-catalyst for CO_2 conversion reaction, which is to prepare various cyclic carbonates from CO_2 and the corresponding epoxides. The yields of the relevant reactions catalyzed by **PIM-1-AI** are range from 87 % to 99 % at 2.5 MPa and 90 °C. **PIM-1-AO** with amidoxime groups is soluble in DMF and was futher fabricated into film and foam-supportting composite to furnish two intgreted adsorbents for uranium uptake in real seawater. By contrast, **PIM-1-AO** film has the highest uranium uptake ability (180.3 mg g^{-1}) tested in real seawater with evaluated uranium (7.98 ppm) at the pH of 8.2 and room temperature. The foam-supportting **PIM-1-AO** can shorten the balance time from 12 to 4 h compared to **PIM-1-AO** film. Moreover, both **PIM-1-AO** film and foam-supporting **PIM-1-AO** as integrated adsorbents can be reused at least 5 times and retain their mass stability meeting the need of practical application for uranium uptake.

Conflicts of interest

There are no conflicts to declare.

Acknowledgements

The financial support of the Finance Science and Technology Project of Hainan Province (No. ZDYF2018004), the National Natural Science Foundation of China (Grants 21574031, 51873053, 61761016 and 51775152), and the Start-up Scientific Research Foundation of Hainan University (Grant KYQD(ZR)1812) is acknowledged.

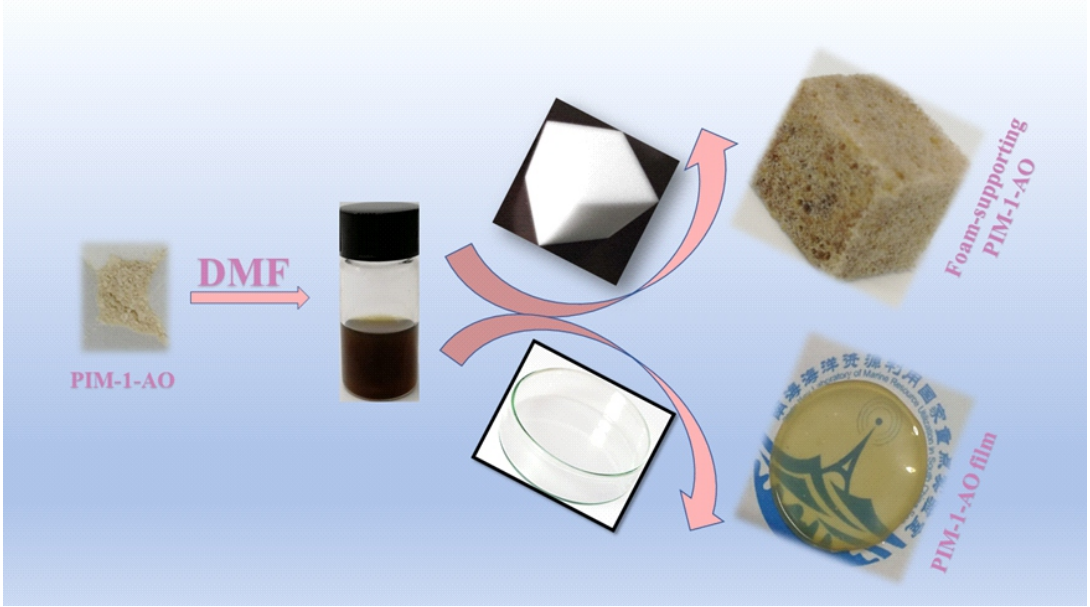

Scheme 2. The **preparation routes** to **PIM-1-AO** firm and **foam-supporting PIM-1-AO.**

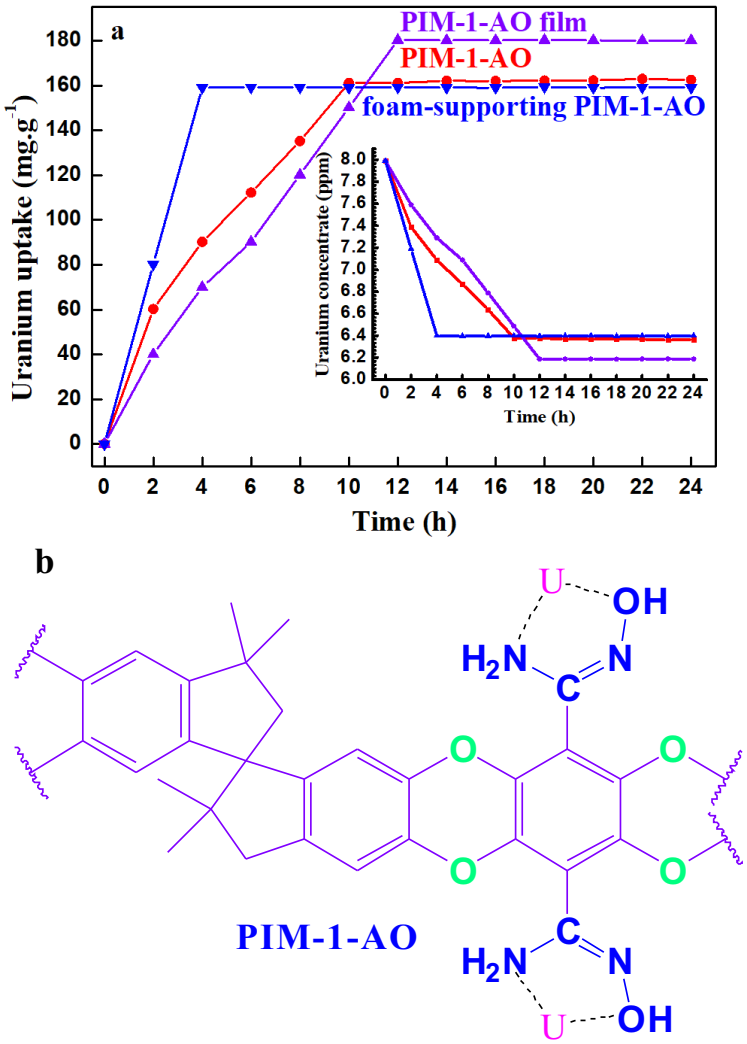

Fig. 5 (a) Uranium uptake isotherm for **PIM-1-AO**, **PIM-1-AO** film and foam-supporting **PIM-1-AO**, measured in the real seawater containing excess uranium (7.98 ppm) at the pH of 8.2, and the inset is the corresponding uranium concentration during the extraction procedure. **(b)** The chelating schema of **PIM-1-AO** for uranium.

References

1. J. Artz, T. Müller, K. Thenert, J. Kleinekore, R. Meys, A. Sternberg, A. Bardow and W. Leitner, *Chem. Rev*., 2017, **118**, 434-504.
2. R. Dawson, E. Stöckel, J. Holst, D. Adams and A. Cooper, *Energ. Environ. Sci.*, 2011, **4**, 4239-4245.
3. E. Sanz-Perez, C. Murdock, S. Didas and C. Jones, *Chem. Rev.*, 2016, **116**, 11840-11876.
4. J. Yu, L. Xie, J. Li, Y. Ma, J. Seminario and P. Balbuena, *Chem. Rev.*, 2017, **117**, 9674-9754.
5. G. Kupgan, L. Abbott, K. Hart and C. Colina, *Chem. Rev.*, 2018, **118**, 5488-5538.
6. S. Hou and B. Tan, *Macromolecules*, 2018, **51**, 2923-2931.
7. Q. Chen, D. Liu; M. Luo, L. Feng, Y. Zhao and B. Han, *Small*, 2014, **10**, 308-315.
8. Q. Chen, D. Liu, J. Zhu and B. Han, *Macromolecules*, 2014, **47**, 5926-5931.
9. M. Aresta and A. Dibenedetto, *Catal. Today*, 2004, **98**, 455–462.
10. Y. Xie, T. Wang, X. Liu, Z. Kun and W. Deng, *Nat. Commun.*, 2013, **4**, 1960.
11. P. Li, X. Wang, J. Liu, J. Lim, R. Zou and Y. Zhao, *J. Am. Chem. Soc.*, 2016, **138**, 2142-2145.
12. M. Wilhelm, M. Anthofer, M. Cokoja M. Cokoja, I. Markovits, W. Herrmann and F. Kühn, *ChemSusChem*, 2014, **7**, 1357-1360.
13. R. Ma, L. He and Y. Zhou, *Green Chem*., 2016, **18**, 226–231.
14. A. Decortes, A. Castilla and A. Kleij, Angew. *Chem., Int. Ed.*, 2010, **49**, 9822–98372.
15. W. Wang, S. Wang, X. Ma and J. Gong, *Chem. Soc. Rev.*, 2011, **40**, 3703–3727.
16. Y. Li, R. Ma, L. He and Z. Diao, *Catal. Sci. Technol.,* 2014, **4**, 1498–1512.
17. Q. Liu, L. Wu, R. Jackstell and M. Beller, *Nat. commun*., 2015, **6**, 5933.
18. Q. Song, Z. Zhou and L. He, *Green Chem.*, 2017, **19**, 3707-3728.
19. C. Martin, G. Fiorani and A. Kleij, *ACS Catal.*, 2015, **5**, 1353-1370.
20. J. Rintjema, R. Epping, G. Fiorani, E. Martin, E. Escudero-Adan and A. Kleij, *Angew. Chem., Int. Ed.*, 2016, **55**, 3972–3976.
21. T. Ema, Y. Miyazaki, J. Shimonishi, C. Maeda and J. Hasegawa, *J. Am. Chem. Soc.*, 2014, **136**, 15270–15279.
22. V. Laserna, G. Fiorani, C. Whiteoak, E. Martin, E. Escudero-Adan and A. Kleij, *Angew. Chem., Int. Ed.*, 2014, **53**, 10416-10419.
23. C. Maeda, T. Taniguchi, K. Ogawa and T. Ema, *Angew. Chem., Int. Ed.*, 2015, **54**, 134–138.
24. J. Hull, Y. Himeda, W. Wang, B. Hashiguchi, R. Periana, D. Szalda, J. Muckerman and E. Fujita, *Nat. Chem.*, 2012, **4**, 383–388.
25. J. Hu, J. Ma, Q. Zhu, Q. Qian, H. Han, Q. Mei and B. Han, *Green Chem.*, 2016, **18**, 382–385.
26. M. Jeletic, M. Mock, A. Appel and J. Linehan, *J. Am. Chem. Soc.*, 2013, **135**, 11533–11536.
27. L. Zhang, Z. Han, X. Zhao, Z. Wang and K. Ding, *Angew. Chem., Int. Ed.*, 2015, **54**, 6186–6189.
28. Z. Xin, C. Lescot, S. Friis, K. Daasbjerg and T. Skrydstrup, *Angew. Chem., Int. Ed.*, 2015, **54**, 6862–6866.
29. X. Frogneux, E. Blondiaux, P. Thuéry and T. Cantat, *ACS Catal.*, 2015, **5**, 3983–3987.
30. E. Blondiaux, J. Pouessel and T. Cantat, *Angew. Chem., Int. Ed.*, 2014, **53**, 12186–12190.
31. Z. Yang, L. He, Y. Zhao, B. Li and B. Yu, *Energy. Environ. Sci.*, 2011, **4**, 3971–3975.
32. J Chen, H. Li, M. Zhong and Q. Yang, *Green Chem.*, 2016, **18**, 6493−6500.
33. J. Chen, M. Zhong, L. Tao, L. Liu, S. Jayakumar, C. Li, H. Li and Q. Yang, *Green Chem.*, 2018, **20**, 903−911.
34. S. Wang, K. Song, C. Zhang, Y. Shu, T. Li and B. Tan, *J. Mater. Chem. A*, 2017, **5**, 1509−1515.
35. G Ji, Z. Yang, H. Zhang, Y. Zhao, B. Yu, Z. Ma and Z. Liu, *Angew. Chem., Int. Ed.*, 2016, **55**, 9685−9689.
36. S. Chu and A. Majumdar, *Nature*, 2012, **488**, 294–303.
37. D. Sholl and R. Lively, *Nature*, 2016, **532**, 435-438.
38. D. Guan, J. Meng, D. Reiner, N. Zhang, Y. Shan, Z. Mi, S Shao, Z. Liu, Q. Zhang and S. Davis, *Nat. Geosci.*, 2018, **11**, 551–555.
39. M. Xu, X. Han, T. Wang, S. Li and D. Hua, *J. Mater. Chem. A*, 2018, **6**, 13894-13900.
40. R. Davies, J. Kennedy, R. Mcllroy, R. Spence and K. Hill, *Nature*, 1964, **203**, 1110-1115.
41. C. Abney, R. Mayes, T. Saito, S. Dai, *Chem. Rev.*, 2017, **117**, 13935-14013.
42. C. Liu, P. Hsu, J. Xie, J. Zhao, T. Wu, H. Wang, W. Liu, J. Zhang, S. Chu and Y. Cui, *Nat. Energ.,* 2017, **2**, 17007.
43. L. Ling and W. Zhang, *J. Am. Chem. Soc.*, 2015, **137**, 2788-2791.
44. D. Wang, J. Song, J. Wen, Y. Yuan, Z. Liu, S. Lin, H. Wang, H. Wang, S. Zhao, X. Zhao, M. Fang, M. Lei, B. Li, N. Wang, X. Wang and H. Wu, *Adv. Energy Mater*., 2018, DOI: 10.1002/aenm.201802607
45. K. Tian, J. Wu and J. Wang, *Radiochim. Acta.,* 2018, DOI: 10.1515/ract-2017-2913.
46. L. Feng, S. Zhang, X. Sun, Dong A and Q. Chen, *J. Mater. Sci.*, 2018, **53**,15025–15033.
47. J. Zhu, Q. Chen, Z. Sui, L. Pan, J. Yu and B. Han, *J. Mater. Chem. A*, 2014, **2**, 16181-16189.
48. P. Burns, R. Ewing and A. Navrotsky, *Science*, 2012, **335**, 1184-1188.
49. A. Ladshaw, A. Lvanov, S. Das, V. Bryantsev, C. Tsouris and S. Yiacoumi, *ACS Appl. Mater. Inter.*, 2018, **10**, 12580-12593.
50. Q Sun, B. Aguila, J. Perman, A. S. Ivanov, V. Bryantsev, L. Earl, C. Abney, L. Wojtas and S. Ma, *Nat. Commun.*, 2018, **9**, 1644.
51. Q. Sun, B. Aguila, L. Earl, C. Abney, L. Wojtas, P. Thallapally and S. Ma, *Adv. Mater*., 2018, **30**, 1705479.
52. G. Cheng, B. Bonillo, R. Sprick, D. Adams, T. Hasell and A. Cooper, *Adv. Funct. Mater.*, 2014, **24**, 5219-5224.
53. R. Dawson, A. Cooper and D. Adams, *Prog. Polym. Sci.*, 2012, **37**, 530-563.
54. H. Yin, Y. Chua, B. Yang, C. Schick, W. Harrison, P. Budd, M. Bohning and A. Schonhals, *J. Phys. Chem. Lett.*, 2018, **9**, 2003-2008.
55. Q. Chen and B. Han, *Macromol. Rapid Commun.*, 2018, **39**, 1800040.
56. Q. Chen, M. Luo, P. Hammershøj, D. Zhou, Y. Han, B. Laursen, C. Yan and B. Han, *J. Am. Chem. Soc*., 2012, **134**, 6084-6087.
57. H. Liang, Q. Chen and B. Han, *ACS Catal.*, 2018, **8**, 5313-5322.
58. P. Budd, E. Elabas, B. Ghanem, N. McKeown, K. Msayjb, C. Tattershall and D. Wang, *Adv. Mater.*, 2004, **16**, 456-459.
59 A. Hasmukh and T. Cafer, *Chem. Commun*., 2012, **48**, 9989–9991.
60 N. Du, G. Robertson, J. Song, I. Pinnau and M. Guiver, *Macromolecules*, 2009, **42**, 6038–6043.
61. N. Du, H. Park, G. Robertson, M. Dal-Cin, T. Visser, L. Scoles

and M. Guiver, *Nat*. *Mater*., 2011, **10**, 372-375.
62. Q. Sun, Y. Zhang, C. Abney, B. Aguila, W. Lin, and S. Ma. *ACS Appl. Mater. Inter.*, 2017, **9**, 12511−12517.
63. Z. Bai, L. Yun, L. Zhu, Z. Liu, S. Chu, L. Zheng, J. Zhang, Z. Chai and W. Shi, *J. Mater. Chem. A*, 2015, **3**, 525-534.
64. H. Patel and C. Yavuz, *Chem. Commun.*, 2012, **48**, 9989-9991.
65. K. Sing, D. Everett, R. Haul, L. Moscou, R. Pierotti, J. Rouquérol and T. Siemieniewska, *Pure Appl. Chem.*, 1985, **57**, 603-619.
66. A. Dong, D. Wang, T. Dai, Q. Chen, L. Feng and N. Wang, *Adv*. *Compos*. *Hybrid Mater*., 2018, DOI: 10.1007/s42114-018-0063-0.
67. A. Zhang, T. Asakura and G. Uchiyama, *React. Funct. Polym.*, 2013, **57**, 67-76.
68. Y. Qian, Y. Yuan, He Wang, H. Liu, J Zhang, S. Shi, Z. Guo and N. Wang, *J. Mater. Chem. A*, 2018, DOI: 10.1039/C8TA09486A.
69. S. Vukovic, L. Watson, Kang, S. Kang, R. Custelcean and B. Hay, *Inorg. Chem.*, 2012, **51**, 3855-3859.